Atmospheric Research 96 (2010) 421–435

Contents lists available at ScienceDirect

Atmospheric Research

journal homepage: www.elsevier.com/locate/atmos

Aerosol size distribution in precipitation events in León, Spain

Amaya Castro, Elisabeth Alonso-Blanco, Miguel González-Colino, Ana I. Calvo, María Fernández-Raga, Roberto Fraile *

Department of Physics, IMARENAB, University of León, 24071 León, Spain

ARTICLE INFO

Article history:
Received 4 December 2008
Received in revised form 28 October 2009
Accepted 31 January 2010

Keywords:
Aerosol optical counter
Aerosol size distribution
Precipitation
Accumulation mode
Coarse mode

ABSTRACT

Precipitation and continuous particle number size distributions have been measured using a passive cavity aerosol spectrometer probe PCASP-X, in an urban environment: the city of León, Spain. Five rain events have been analyzed in detail, none of which registered very intense precipitation, ranging from 2.5 mm to 14.7 mm, with a maximum rain intensity of 5.6 mm/h. The study focuses on the influence of precipitation in aerosol size distributions before, during and after a rain event. Washout effects have been observed during rain events with intensities of over 3.2 ± 1.5 mm/h, resulting in a decrease of 20% in the number of particles detected, the decrease affecting large and small particles alike. However, if the rain intensity is about 0.6 mm/h or lower, the result is a considerable increase in the number of aerosols measured — up to 89% more — with an increase in the number of particles smaller than 1.3 μm and a decrease in the number of particles larger than 1.3 μm. It may be the case that during very weak rain intensity the probe does not discriminate adequately between aerosols and small precipitating droplets or the extremely small droplets that remain in suspension in the atmosphere. In consequence, it will be argued that measurements taken during very weak rain events (with an intensity of less than 0.6 mm/h), such as drizzle or dense fog, should be treated separately or not be considered. The performance of the accumulation and coarse modes has also been studied, as well as the count median diameters (CMDs) before, during and after the rain event.

1. Introduction

The size distribution of atmospheric aerosols strongly depends on the sources and sinks as well as on the meteorological processes prevailing during their lifetime (Suzuki and Tsunogai, 1988; Ito, 1993). In studying aerosol size distributions we must take into account, on the one hand, the type of air mass and the anthropogenic or natural contributions that may have affected that air mass, and on the other hand, the hygroscopic properties of the aerosols and the aerosol–precipitation interaction in the elimination of aerosols through precipitation.

The ability of atmospheric aerosol particles to absorb water is a feature of prime importance, but the study of this characteristic is a complex task (Kerminen 1997). This ability has many consequences because the particulate water content affects the size and total mass of particles, their acidity, the amount of water-soluble substances they contain, their light-scattering and absorbing properties, their chemical reactivity, their effectiveness acting as cloud condensation nuclei, and their atmospheric lifetime. Thus, variations in aerosol concentration may be seen as one of the causes of precipitation or as one of its consequences (Teller and Levin, 2006; Jirak and Cotton, 2006). The ability to absorb water can be highly variable and depends on sub-micrometer particles of internal mixtures of inorganic and organic material (Cocker et al. 2001; Väkevä et al., 2002; Aklilu et al. 2006).

Authors such as Slinn (1971) or Dana and Hales (1976) established theoretically the linear relationships between the scavenging coefficient and rain intensity for different aerosol types and this may be used to describe the time variation of

* Corresponding author.
E-mail address: roberto.fraile@unileon.es (R. Fraile).

0169-8095/$ – see front matter © 2010 Elsevier B.V. All rights reserved.
doi:10.1016/j.atmosres.2010.01.014

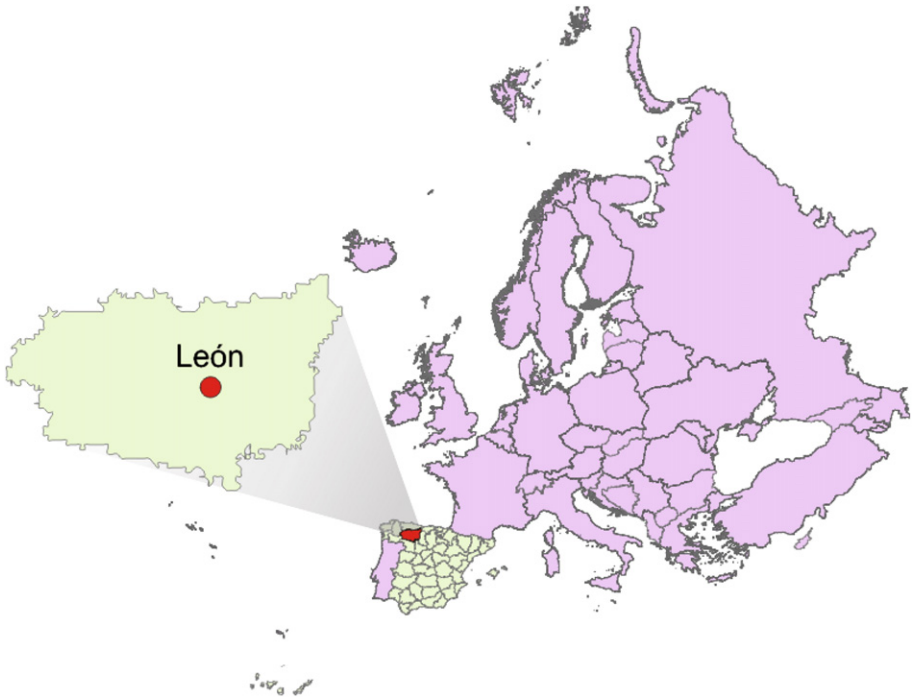

Fig. 1. Geographic location of the city of León, Spain.

mass/number concentration of pollutants in the atmosphere. Other authors such as Mircea et al. (2000), Dana (1971) and Dana (1972) obtained experimental data showing that below-cloud scavenging is much more efficient for the polydisperse aerosol than might be expected for particles with a specified mean size.

Optical particle counters (OPCs) are used for *in situ* measurements of particle size and concentration of atmospheric aerosols (Collins et al. 2000, Guyon et al. 2003). OPCs measure the magnitude of light scattering by individual aerosol particles and then use an internal calibration function to determine their size. These instruments are usually calibrated using latex particles with a refractive index $m = 1.588 - 0i$. These particles are highly efficient scattering radiation, as indicated by the large real component of the refractive index, and they are completely non-absorbing (no imaginary component). But aerosol particles behave differently: they are usually less efficient radiation scatterers and display absorptive properties. Therefore, OPCs present measuring problems and corrections must be made depending on the refractive index of the particles that are being measured.

The type of aerosol that is being measured must be determined because urban, rural or maritime aerosols or air masses with a mixture of different types of aerosols behave in completely different ways in the probes when the light beam falls on them. The refractive index of the particles must be known, since scattering (real component) and absorption (imaginary component) combined will account for the different responses on the optical properties of the probes used (Hinds, 1999).

In addition, aerosol light-scattering is usually interpreted in dry conditions with relative humidities (RHs) lower than 30–40%, conditions that differ a lot from many environmental situations when the measurements might have taken place. Many ambient aerosols undergo hygroscopic growth at enhanced relative humidity, and their microphysical (particle size) and optical properties (refractive index) are strongly dependent on relative humidity. Determining the organic and inorganic fraction of aerosols is also important, as well as establishing their ability to take up water (Swietlicki et al., 1999; Peng et al., 2001; Busch et al., 2002). If the probe is used to measure the size distribution of aerosol particles encountered during airborne measurements in the lower troposphere under different atmospheric conditions, several authors such as Kim and Boatman (1990) suggest that the relative humidity must be considered and the aerosols must be assigned a refractive index corrected taking ambient humidity into account.

Aerosol size distribution influences the dynamics of aerosol population (Väkeva et al., 2000), their production and removal processes, size transformation, lifetime, optical properties and radiative effects (Huebert et al. 1996). Authors such as Kerminen and Wexler (1995) try to explain the frequently observed splitting of the accumulation mode into two individual modes by analyzing the growth of atmospheric aerosol particles considering all important aerosol processes: condensation, coagulation, aqueous-phase reactions in droplets or aerosol particles, and reactions taking place at the interface of two phases.

The present study is an attempt to relate the air masses causing precipitation in León to aerosol size distribution in order to analyze changes in aerosol size distributions during rain events. When there is rain, the ambient conditions vary at surface level. This study will analyze the performance of an OPC measuring aerosol size distributions before, during and after precipitation, and especially in situations of very weak precipitation.

Table 1
Mean diameters of the 31 channels of the PCASP-X probe between 0.1 and 10 μm for the manufacturer's calibration with polystyrene latex beads ($m=1.59-0i$) and mean diameters corrected for urban aerosols in a dry atmosphere ($m=1.56-0.087i$) and for urban aerosols in a very humid atmosphere ($m=1.384-0.0194i$). Midpoint latex diameter and midpoint for dry and humid urban aerosols diameter ratio ($\tau_{latex}/\tau_{aerosol}$) are also shown.

Channel PCASP-X	Range diameter			$\tau_{latex}/\tau_{aerosol}$	
	Polystyrene latex	Urban aerosols	Urban aerosols		
	$m=1.588-0i$	RH = 50% $m=1.56-0.087i$	RH = 90% $m=1.384-0.0194i$	(a)	(b)
		(a)	(b)		
1	0.10–0.12	0.08–0.10	0.10–0.12	1.22	1.00
2	0.12–0.14	0.10–0.12	0.12–0.14	1.18	1.00
3	0.14–0.16	0.12–0.14	0.14–0.17	1.15	0.94
4	0.16–0.18	0.14–0.16	0.17–0.19	1.13	0.94
5	0.18–0.20	0.16–0.17	0.19–0.21	1.12	0.95
6	0.20–0.23	0.17–0.20	0.21–0.24	1.13	0.93
7	0.23–0.26	0.20–0.22	0.24–0.27	1.17	0.94
8	0.26–0.30	0.22–0.25	0.27–0.31	1.17	0.97
9	0.30–0.35	0.25–0.29	0.31–0.44	1.20	0.86
10	0.35–0.40	0.29–0.36	0.44–0.55	1.14	0.75
11	0.40–0.45	0.36–0.43	0.55–0.64	1.06	0.71
12	0.45–0.50	0.43–0.52	0.64–0.74	0.99	0.69
13	0.50–0.60	0.52–0.72	0.74–0.95	0.89	0.65
14	0.60–0.70	0.72–2.02	0.95–1.08	0.47	0.64
15	0.70–0.80	2.02–2.30	1.08–1.17	0.35	0.66
16	0.80–0.90	2.30–2.64	1.17–1.27	0.34	0.70
17	0.90–1.00	2.64–2.99	1.27–1.37	0.34	0.72
18	1.00–1.20	2.99–3.34	1.37–1.47	0.35	0.77
19	1.20–1.40	3.34–3.70	1.47–1.85	0.37	0.78
20	1.40–1.60	3.70–4.06	1.85–2.36	0.39	0.71
21	1.60–1.80	4.06–4.46	2.36–2.95	0.40	0.64
22	1.80–2.00	4.46–4.96	2.95–3.80	0.40	0.56
23	2.00–2.30	4.96–5.67	3.80–5.41	0.40	0.47
24	2.30–2.60	5.67–6.53	5.41–7.25	0.40	0.39
25	2.60–3.00	6.53–7.29	7.25–9.11	0.41	0.34
26	3.00–3.50	7.29–8.10	9.11–10.90	0.42	0.32
27	3.50–4.00	8.10–9.46	10.90–13.62	0.43	0.31
28	4.00–5.00	9.46–11.72	13.62–17.55	0.42	0.29
29	5.00–6.50	11.72–14.90	17.55–22.68	0.43	0.29
30	6.50–8.00	14.90–18.05	22.68–27.89	0.44	0.29
31	8.00–10.00	18.05–21.98	27.89–35.09	0.45	0.29

The changes in the accumulation mode and the coarse mode when the probe is measuring during a rain event will also be studied in situations of more or less intense precipitation. Changes in the size of the particles measured according to hygroscopic growth, collisions with other particles or raindrops will also be analyzed.

2. Study zone

The measurements were performed in León, Spain, a city in the northwest of the Iberian Peninsula (42º 36′ N, 05º 35′ W and 838 m above sea level) shown in Fig. 1. Because of the absence of large emitting industries, the main source of particulate emissions is considered to be vehicular traffic. León has a population of about 135,000 inhabitants. The weather in León is monitored by the station of the Spanish National Agency of Meteorology installed at the airport of La Virgen del Camino, 6 km from León.

In León the climate is of the Mediterranean type with continental features, somewhat tempered by the proximity of the Cantabrian Mountain Range to the north. Rain events are scattered irregularly over the year, with minimum precipitation values in the summer and maximum values in spring and fall. The annual mean precipitation is 556 mm. On average there are 2624 sun hours per year, 78 rain days and 16 storm days. The temperatures are fresh, with an annual mean of 10.9 °C; the winter is cold and there are frequent frosts (74 frost days per year, on average). On average there are 16 snow days in the city of León, but large snowfalls are not frequent. The summer is warm, but tempered by the altitude of the city, with maximum temperatures around 27 °C.

3. Materials and methods

The study period comprises the 59 days of the months of February and March 2005. The precipitation was collected by the rain gauge of a Davis weather station. The data were registered every 15 min and the minimum volume was 0.25 liters per square meter. The weather station and the aerosol probe were installed at the same site to the southwest of the city of León, Spain. The weather station also provided information on relative humidity, measuring on average 90% of humidity at the sample point during rain events. Three days of precipitation were observed in February and five in March, although only 5 of these days were analyzed in detail, when the total precipitation for the day was in excess of 2.5 mm.

Continuous particle number size distributions were measured using a passive cavity aerosol spectrometer probe: PCASP-X, manufactured by Particle Measuring Systems, Inc. (PMS). This instrument measures aerosol size distribution of diameters ranging between 0.1 and 10 μm in 31 channels on the basis of the light-scattering properties of the particles at a wavelength of 633 nm between angles of 35º and 135º. The probe was calibrated by the manufacturer using polystyrene latex particles of a known size. The refractive index of latex beads ($1.588-0i$) is different from that of atmospheric particles, resulting in an aerosol size distribution that is "latex equivalent." In this paper we are presenting PCASP-X size distributions corrected using Mie theory and implemented with a computer code developed by Bohren and Huffman (1983) for an average refractive index of $m=1.56-0.087i$ (relative humidity around 50%), typical of urban aerosols (Lide, 1993). During the rain events the size distributions are corrected for a refractive index of urban

Table 2
Meteorological study of the months of February and March 2005 with data on maximum, minimum and average temperatures, relative humidity, total precipitation registered and wind intensity.

	February	March
T_{min} (°C)	−5.6	−8.5
T_{max} (°C)	17.9	21.9
T_{av} (°C)	3.8	8.1
Relative humidity (%)	60.2	56.1
Total precipitation (mm)	15.9	31.9
Wind (m/s)	1.0	1.7

Table 3
Meteorological values of the days where a rain event was analyzed: maximum, minimum and average temperature, relative humidity, wind intensity, and total precipitation of each day. For the rain events studied the following data are added: time interval (Δt), precipitation (P) and maximum rain intensity (R).

Date	Day						Event		
	T_{max} (°C)	T_{min} (°C)	T_{av} (°C)	HR (%)	Wind (m/s)	P_{total} (mm)	Δt (UTC)	P (mm)	R_{max} (mm/h)
06/02/2005	5.2	1.4	2.8	80.1	0.0	10.9	1130–2300	10.6	3.0
22/02/2005	3.9	1.6	2.4	84.0	5.9	2.5	0645–0915	2.5	2.0
20–21/3/2005	15.3	10.6	11.7	83.6	1.2	9.3	1815–0530	7.5	2.0
25/03/2005	12.3	8.0	9.3	82.6	3.9	3.8	1100–1330	2.8	3.0
26/03/2005	7.3	6.6	6.9	90.4	2.7	14.7	0100–0600	12.2	5.6

aerosols in an environment with a relative humidity around 90% ($m=1.384-0.0194i$, following Kim and Boatman (1990)). This value is close to the refractive index of water ($m=1.33-0.0i$). A sample was taken every half hour. The sampling process lasted 15 min, and the data were recorded every minute.

After correction, the mean particle size range changed from 0.1–10 μm (nominal range of the PCASP) for the refractive index of latex particles ($1.588-0i$) to 0.1–21.98 μm and 0.1–35.09 μm for $m=1.56-0.087i$ and $m=1.384-0.0194i$, respectively. Table 1 shows the mean diameters in each channel for the different refractive indices. It can be seen that from channel 12 and channel 3 onwards, respectively, the probe tends to underestimate the size of urban aerosol particles due to the effects of particulate absorption. The magnitude of the sizing differences increases as the refractive index deviates from that of the manufacturer's calibration with latex particles and with ambient humidity.

The multi-lognormal function has been used to characterize the size distributions of aerosol particles (e.g. Whitby, 1978; Hoppel et al., 1994). Several data sets of aerosol particles may so be compared easily. The multi-lognormal concept is thoroughly described in the literature and the overall outcome has proven to be useful whenever parameterizations are required (e.g. Mäkelä et al., 2000; Birmili et al., 2001). The particle size distribution is assumed to consist of several lognormal modes:

$$\frac{dN(D)}{d\left(log\left(D_p\right)\right)} = \sum_{i=1}^{n} \frac{N_i}{\sqrt{2\pi}log\left(\sigma_{g,i}\right)} exp\left[-\frac{\left(log\left(D_p\right)-log\left(\overline{D}_{pg,i}\right)\right)^2}{2\left(log\sigma_{g,i}\right)^2}\right]$$

The three parameters that characterize an individual mode i are: the mode number concentration N_i (cm^{-3}); the mode geometric variance $\sigma^2_{g,i}$ (dimensionless), and the mode geometric mean diameter $\overline{D}_{pg,i}$ (μm). D_p is the particle diameter and n is the number of individual modes. The least-square method was used to estimate the lognormal parameters N_i, σ_{gi}, and $\overline{D}_{pg,i}$ (Hussein et al., 2005). In the case of surface and volume distribution, in the previous formula the number of particles, N_i, is replaced by surface area S_i and volume V_i of the particles, respectively.

For the count distribution, the geometric mean diameter, D_g, is customarily replaced by the count median diameter or CMD. The geometric mean is the arithmetic mean of the distribution of log D_p, which is a symmetrical normal distribution, and hence, its mean and median are equal. The median of the distribution of log D_p is also the median of the distribution of D_p, as the order of values does not change in converting to logarithms. Thus, for a lognormal count distribution, $D_g=$ CMD.

Back trajectories of 120 h (5 days) have been used, considered up until the time the rain event began. These back trajectories have been calculated at 500 m, 1500 m and 3000 m AGL employing the HYSPLIT model (*HYbrid Single-Particle Lagrangian Integrated Trajectory Model*) (Draxler and Rolph, 2003) in order to interpret the different source regions of the air masses reaching the study zone. The HYSPLIT model (Draxler and Hess, 1998) carries out a wide range of simulations related to long-range transport, dispersion and deposition of contaminants. The model has been developed by the Air Resources Laboratory of NOAA, Maryland, USA. This study will be complemented by a description of the air masses involved in the rain events.

In order to identify the type of weather associated to a particular synoptic situation a Circulation Weather Types (CWTs) classification was carried out based on Jenkinson and Collison (1977) and Jonses et al. (1993). These procedures were developed to define objectively Lamb Weather Types (LWTs) (Lamb, 1972) for the British Isles. The daily circulation affecting the Iberian Peninsula is described using a set of indices associated to the direction and vorticity of the geostrophic flow. The indices used were the following: southerly flow (SF), westerly flow (WF), total flow (F), southerly shear vorticity (ZS), westerly shear vorticity (ZW) and total shear vorticity (Z). These indices were computed

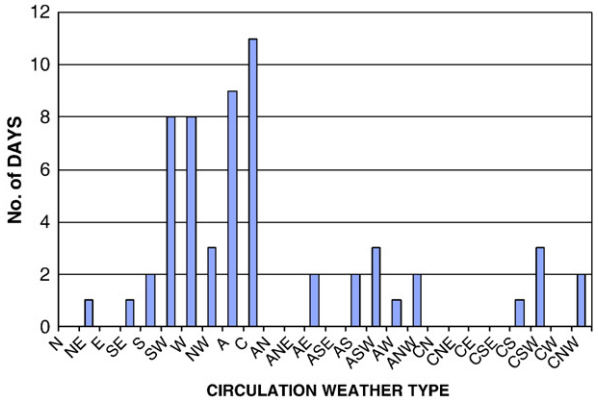

Fig. 2. Circulation Weather Type classification in the months of February and March (59 days).

using sea level pressure values (SLP) obtained for the 16 grid points distributed over the Iberian Peninsula. This method allows for a maximum of 26 different CWTs. Following Trigo and DaCamara (2000) in their study for Portugal, the present study does not make use of a default class for situations that are difficult to group into the main classes, but rather opts for disseminating the fairly few cases with possible unclassified situations (<2%) among the retained classes.

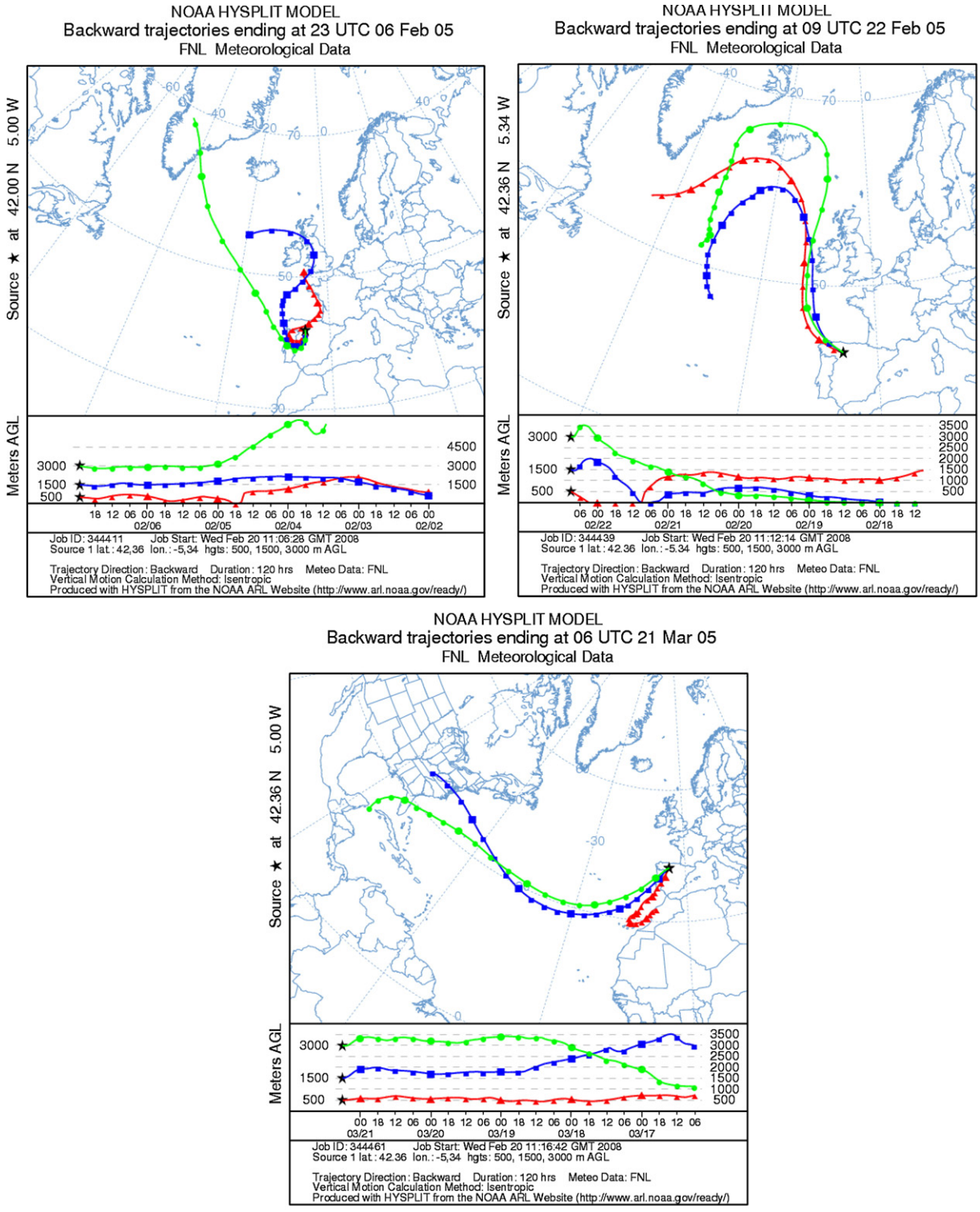

Fig. 3. Back trajectories for three different altitudes (500, 1500 and 3000 m) using the HYSPLIT model.

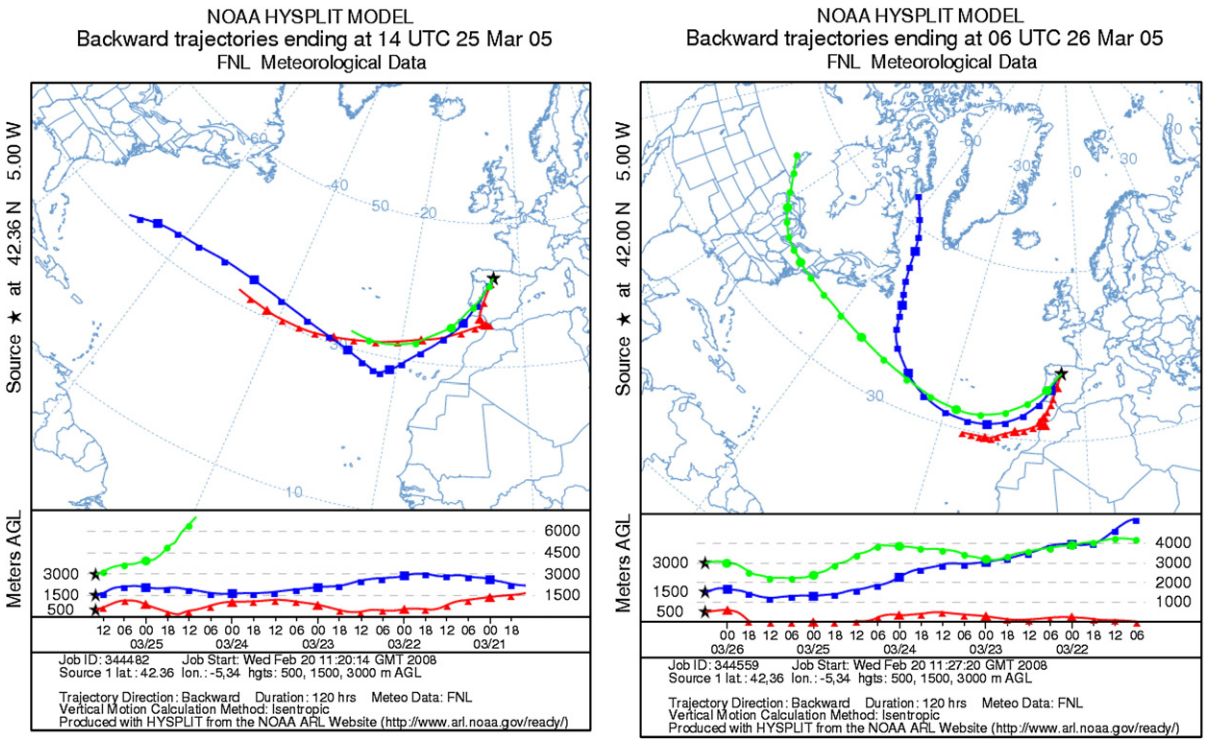

Fig. 3 (*continued*).

For each of the 59 days of observation, the aerosol size distributions were analyzed, as well as the mean geometric diameter and the geometric deviation.

In addition, the distributions corresponding to the five most intense precipitation events in these two months are studied in depth. In these five cases the Circulation Weather Type and the corresponding air masses are also described. The features of the accumulation and coarse modes are studied too for the number of particle distribution, surface and volume distributions in three different stages: before, during and after the rain event.

4. Results and discussion

4.1. Meteorological study

The meteorological study of the two months is shown in Table 2. The average temperatures were typical of winter months and the humidity was about 60%. The rainiest month was March with 8 rain days. In contrast, in February rain was registered only on 3 days and the total precipitation registered was half the one registered in March.

The 5 most intense rain events (with a total precipitation of >2.5 mm) in those two months were studied (Table 3) by analyzing several meteorological parameters such as the duration of the event, the total precipitation registered and the intensity. The relative humidity is remarkably high on these days during the rain events and the wind intensity can be classified according to the Beaufort scale as between calm and moderate breeze for the most intense event with 5.9 m/s. The precipitation registered oscillated between 2.5 mm and 14.7 mm. The events studied on those days lasted between 2 h 30 m and 11 h 30 m. The maximum rain intensity was 5.58 mm/h, and was registered on March 26, i.e., the rain events presented a low intensity.

4.2. Circulation Weather Type and air masses

The Circulation Weather Type classification (CWT) shows that during the months of February and March, (Fig. 2) the CWTs were mainly of two types controlled by geostrophic vorticity: cyclonic (C) and anti-cyclonic (A), with 11 and 9 days, respectively. The next most frequent types were two purely directional types, southwesterly (SW) and westerly (W), followed by the NW, ASW and CSW types. In other words, westerly flows seem to have a strong influence on the Iberian Peninsula in the months of February and March. The weather types during the 5 rain events were: CS on 6 February, SE on 22 February, C-CSW on 20–21 March and SW on 25–26 March.

On the other hand, back trajectories for three different altitudes (500, 1500 and 3000 m) were analyzed to determine the air masses present in the city of León during the days with rain events (Fig. 3). On February 6 and 22 the air masses have been identified as of the maritime Polar (mP) type with low temperatures and a high relative humidity. On March 21 and 25 the air masses were of the maritime Tropical (mT) type and on March 26 of the mP type, with a considerable drop in the temperatures and a remarkable increase in the relative humidity.

So, considering the back trajectories and the weather types of the events analyzed, it may be said that on 6 February in the hours immediately before the rain event the air mass over the city of León had been influenced by the fact that it had

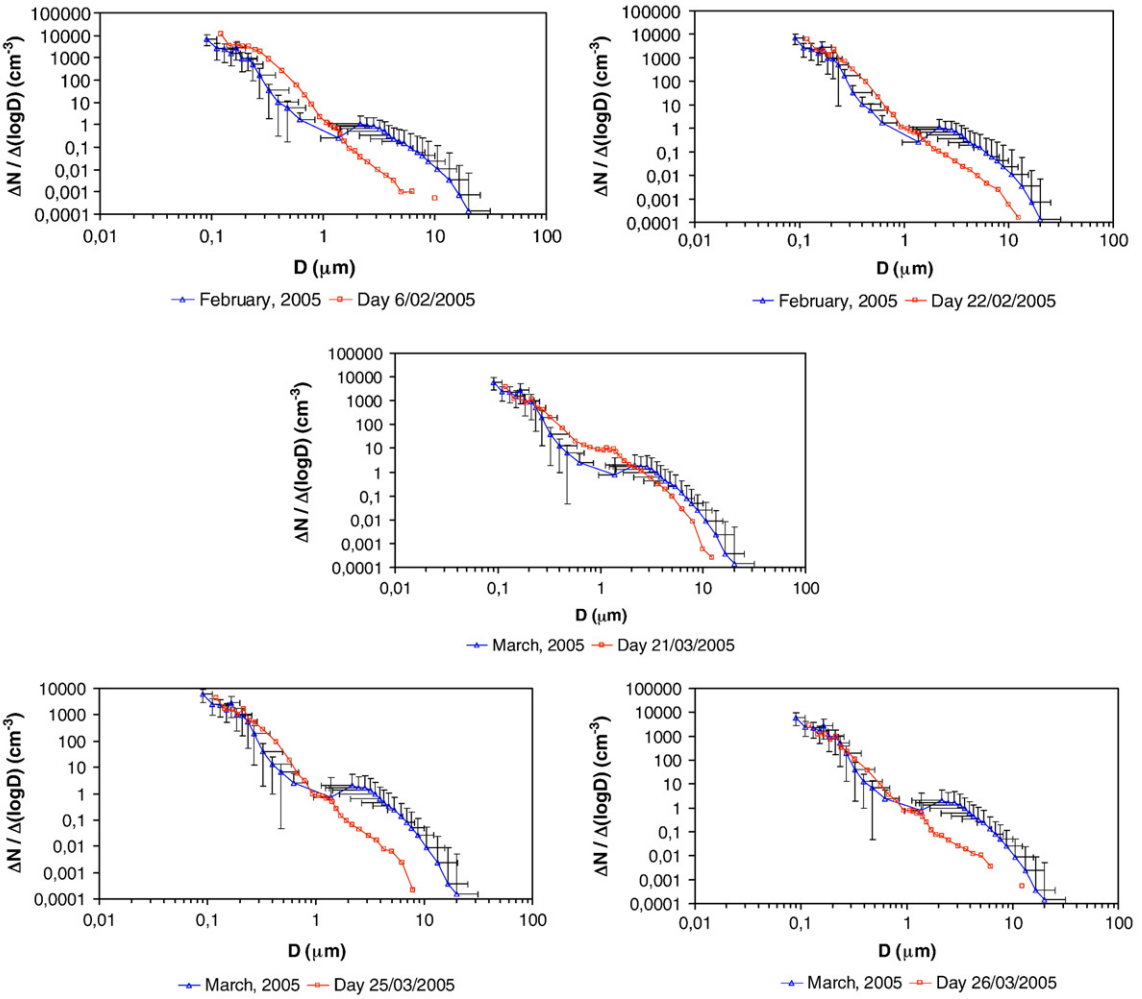

Fig. 4. Average aerosol size distributions in the day with the rain event and in the corresponding month. The vertical error bars represent the standard deviation of the number of particles. The horizontal error bars represent the uncertainty in the size of the aerosol due to the variation of the refraction index between a dry and humid atmosphere.

previously crossed over the rest of the Iberian Peninsula. This air mass stayed over the Peninsula for over 24 h before arriving at León, time enough to incorporate aerosols from natural sources as well as from anthropogenic sources. A number of studies carried out within the framework of the CALIMA Project (Caracterización de AerosoLes originados por Intrusiones de Masas de aire Africanas[1]) determine the contribution of aerosols from biomass burning, sulfates from central Europe and aerosols from northern Africa in the northwest of the Iberian Peninsula (http://www.calima.ws). From the outputs of the forecast models analyzed, that day there was contribution from biomass burning to the levels of particles registered on the ground.

On the other days with rain events in the study period there is no evidence of contribution due to the short period of time the air mass stayed over the Peninsula: hardly 6–12 h. During the event on 20–21 March an intrusion of Saharan dust was detected over the Peninsula, but not in León, and on 22 February the back trajectory at 500 m indicates an approach of the air mass to the surface level, thus favoring the collection of particulate matter from the ground and from aerosol-generating anthropogenic sources. The air masses and their evolution explain the higher or lower number of aerosols that reach the sampling point. As far as the back trajectories are concerned, none of the air masses analyzed presents a sudden change in its characteristics while the precipitation lasts. This must be taken into account when interpreting the results in the following section.

4.3. Influence of the precipitation on aerosol size distribution measurements

In each rain event the evolution of the number of aerosols has been analyzed, as well as the mean geometric diameter and its geometric deviation, in order to detect variations and their development before the actual precipitation was

[1] Characterization of Aerosols from African Air Mass Intrusions.

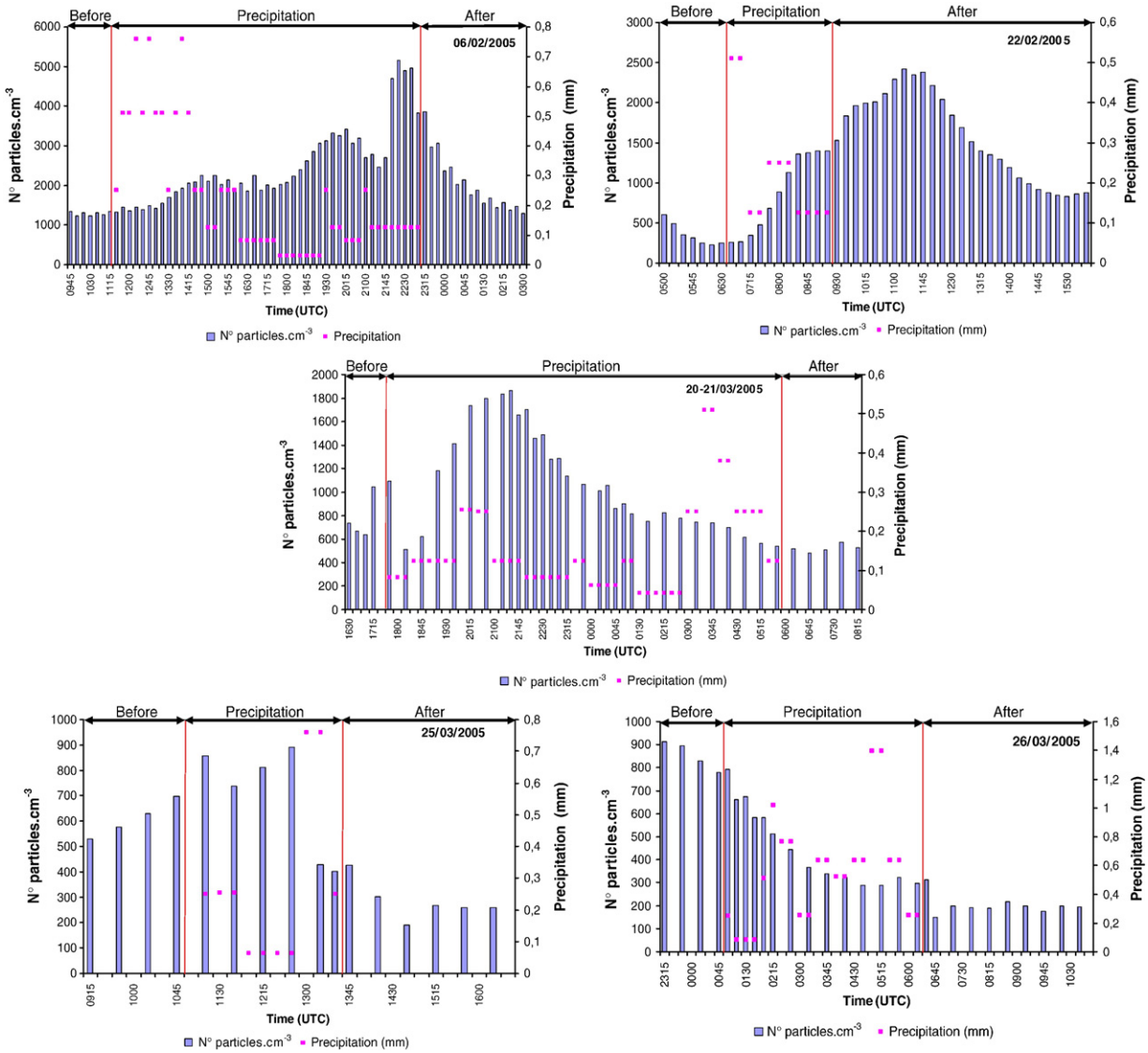

Fig. 5. Time variation of the number of aerosols and the precipitation in the 5 days with rain events. Three stages are distinguished: before, during and after the rain.

registered, during the precipitation, and after the event in intervals of 15 min.

Fig. 4 shows a comparative study of the average distributions of the days with rain events with reference to the month in which they occurred. In the figure, a refraction index of $m = 1.56 - 0.087i$ (RH = 50%) has been used for the days of the month without rainfall. On the days with precipitation, the same index has been used for the simples taken before and during the precipitation. During the rain events, a value of $m = 1.384 - 0.0194i$ (RH = 90%) has been used.

Fig. 4 shows the error bars for each piece of data from the different months. The vertical bars show the geometric deviation in the average number of particles per month. The horizontal bars show the uncertainties in the size due to the possible variation of the refraction index between a dry atmosphere and a very humid atmosphere. On the days with precipitation studied, only the size of the smaller particles at 0.3 μm is overlapped by the error bars. In general, the uncertainty due to the refraction index does not include the values of the mean particle size for any size. The only exception is the 26th of March for sizes of less than 0.8 μm.

The situation varies from one day to another. In general, it has been observed that the number of small particles — smaller than 1 μm — is higher on the days with rain events than the average of the two months of February and March, and conversely, the number of larger particles — larger than 1 μm — is lower on the days with rain events than the average for the two months. Only on 20–21 March the changes are not so important for aerosols larger than 2 μm. A considerable increase in the number of particles is observed on days with rain events, with very different figures to the ones registered on days with no rain in the same month.

Fig. 5 shows the number of particles and the precipitation registered in each 15-minute interval and for each of these

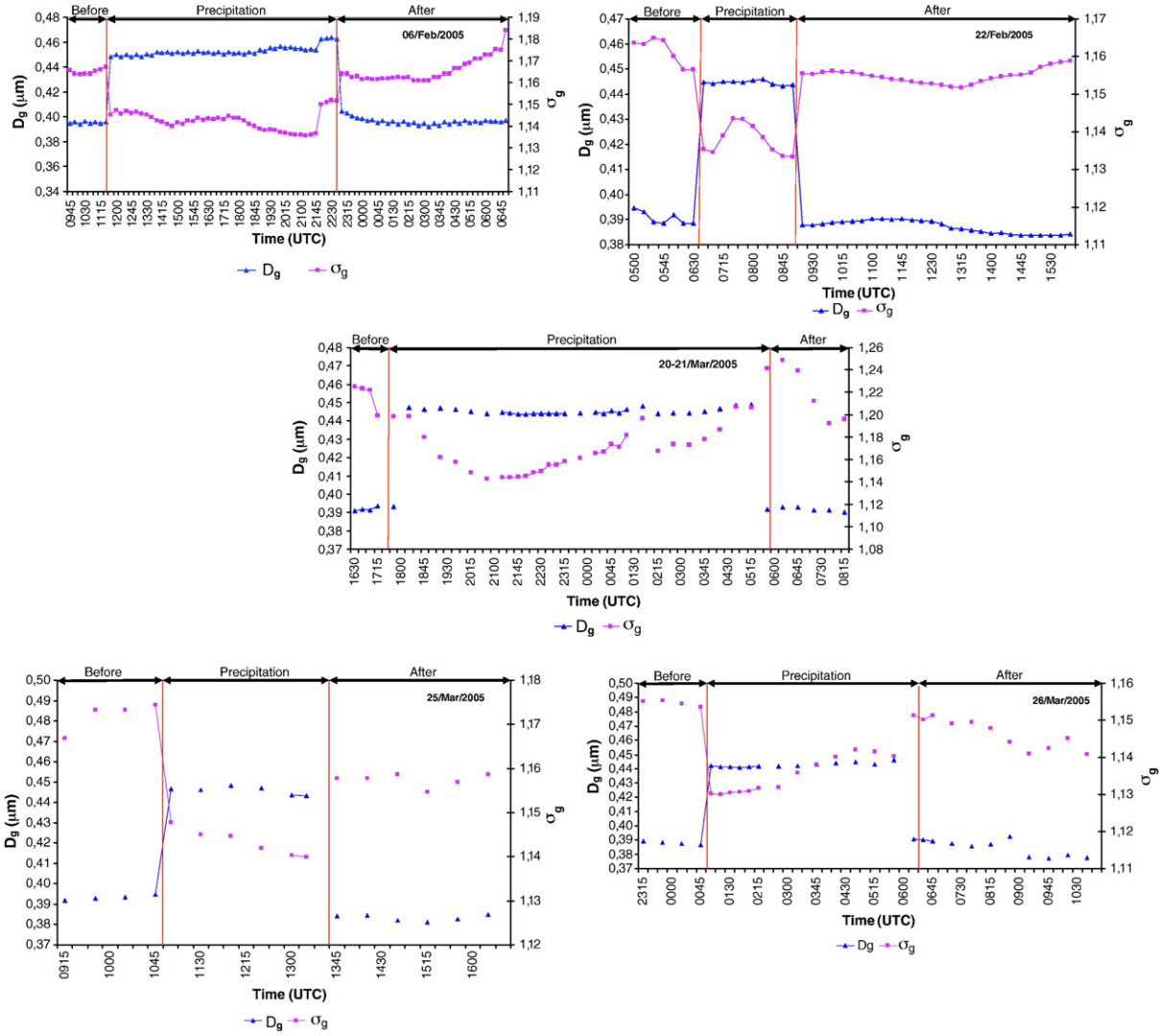

Fig. 6. Time variation of the Count Median Diameter (CMD) and its geometric deviation in the 5 days with rain events. Three stages are distinguished: before, during and after the rain.

intervals the rain intensity have been calculated to assess how the two parameters vary simultaneously. Fig. 6 illustrates the evolution of the mean geometric diameter (based on the number concentration) and its geometric deviation in the 5 days with rain events in three stages: before, during and after the rain. Table 4 includes the characteristics of number size distribution, surface distribution and volume distribution averaged for the 5 events, together with data relative to precipitation and intensity. The computations have been carried out in three intervals: before, during and after the rain event. During the precipitation we have distinguished between the measurement carried out at the moment of maximum precipitation of the day and the remaining measurements taken during the rain event.

In the days analyzed it was found that:

- During the rain event the number of particles detected increases when the intensity of the precipitation is lower than 0.6 mm/h (up to 89% on average, but on 22 February 2005 in certain time intervals increases of over 700% have been observed), and decreases again after the precipitation. However, the initial values are not achieved immediately: even an hour and a half after the rain has ceased the number of particles may still be 20% higher than the ones measured before the rain because the disappearance of the smallest droplets left in suspension takes some time. This delay is due to the fact that after a time the air mass returns to having the initial water content conditions, due to wind action or evaporation processes. But when the precipitation intensity was over 3.2 mm/h, after the rain event there were fewer particles than before the event in a much shorter time span. It was found that after the rain event, if the intensity of the precipitation had been very low, lower than 0.6 mm/h, it took about 2 h for the number of particles to regain values

Table 4
Geometric mean diameter (D_g) and its geometric deviation (σ_g) for (a) number size distribution, (b) surface distribution and (c) volume distribution averaged for the 5 events studied together with data about precipitation and intensity assessed in three stages: before the rain event, during the event (measured at the moment of maximum precipitation and for the remaining measures at other moments during the rain event) and after the precipitation. The table shows each average value with its standard deviation.

		Precipitation (mm)	Rate precipitation (mm/h)	Number size distribution			Surface distribution			Volume distribution		
				N (cm^{-3})	Dg (μm)	σ_g	S ($\mu m^2\ cm^{-3}$)	Dg (μm)	σ_g	V ($\mu m^3\ cm^{-3}$)	Dg (μm)	σ_g
Before		0	0	794 ± 293	0.39 ± 0.002	1.17 ± 0.02	69 ± 55	0.65 ± 0.38	1.56 ± 0.16	22 ± 46	1.29 ± 0.39	1.79 ± 0.28
During Precipitation	Maximum precipitation	0.79 ± 0.36	3.15 ± 1.45	637 ± 499	0.44 ± 0.002	1.15 ± 0.02	67 ± 53	0.56 ± 0.09	1.38 ± 0.12	4 ± 4	0.77 ± .19	1.54 ± 0.17
	Other dates	0.16 ± 0.17	0.62 ± 0.67	1498 ± 1410	0.45 ± 0.01	1.14 ± 0.01	157 ± 163	0.54 ± 0.07	1.33 ± 0.13	8 ± 7	0.71 ± 0.19	1.44 ± 0.09
After		0	0	946 ± 995	0.39 ± 0.004	1.16 ± 0.01	60 ± 55	0.62 ± 0.22	1.72 ± 0.22	9 ± 14	1.42 ± 0.35	1.65 ± 0.20

similar to or lower than the initial number registered before the rain event.

- Only during the maximum intensity of a rain event have we observed a decrease in the number of particles of 20%. In other words, the washout effect is only evident in the case of more intense precipitation, on average 3.2 ± 1.5 mm/h. But if the rain intensity is about 0.6 mm/h or lower, the result is a considerable increase in the number of aerosols measured. It may be the case that during weak rain events the probe does not discriminate adequately between aerosols and small precipitating droplets or extremely small droplets that remain in suspension in the atmosphere. It is important to take into account the fact that the droplets are not only formed by condensation on previously existing condensation nuclei, because in the sampling area, more droplets formed in the upper layers of the atmosphere appear at ground level, while the number of aerosols on the surface will remain constant if there are no changes in the air mass or other sources.

- When the intensity of the precipitation is over 3.2 mm/h, there is an intense washout and the number of particles decreases significantly, large and small particles alike (Fig. 7). In Figs. 7 and 8, a refraction index of $m = 1.56 - 0.087i$ has been used for the samples taken before and during the precipitation. During the rain events, a value of $m = 1.384 - 0.0194i$ has been used. It may be seen in the figures that the shift in size is not justified by the uncertainty of the refraction index (represented by the horizontal error bars).

- When the intensity of the precipitation is lower than 0.6 mm/h we have very light rain and when analyzing the variations in the distributions every 15 min, the number of particles increases considerably, presenting up to seven times the number of particles. The average sizes larger than the ones registered before the beginning of the rain event, growing from 0.39 μm to 0.45 μm (meaning it increases by 15). In other words, there is a lot of variation in the distributions. Fig. 8 shows that under these conditions of precipitation the number of particles smaller than 1.3 μm increases, whereas the number of particles larger than 1.3 μm decreases.

- The mean geometric diameter was 0.39 μm before and after the rain event, and its geometric deviation was 1.16 and 1.17, respectively. This means that the aerosol size distribution regains its initial values approximately 2 h after the precipitation. So, a short time after the precipitation the air mass recovers the same type of distribution it had before the rain event.

- The average particle size increases to diameters of 0.45 μm during the rain event and to 0.44 μm during the periods of maximum intensity. The standard deviations found are very small: lower than 0.01 μm in all cases. A negative correlation has been found between precipitation intensity and the mean geometric diameter, i.e., when it begins to rain the mean diameter of the particles

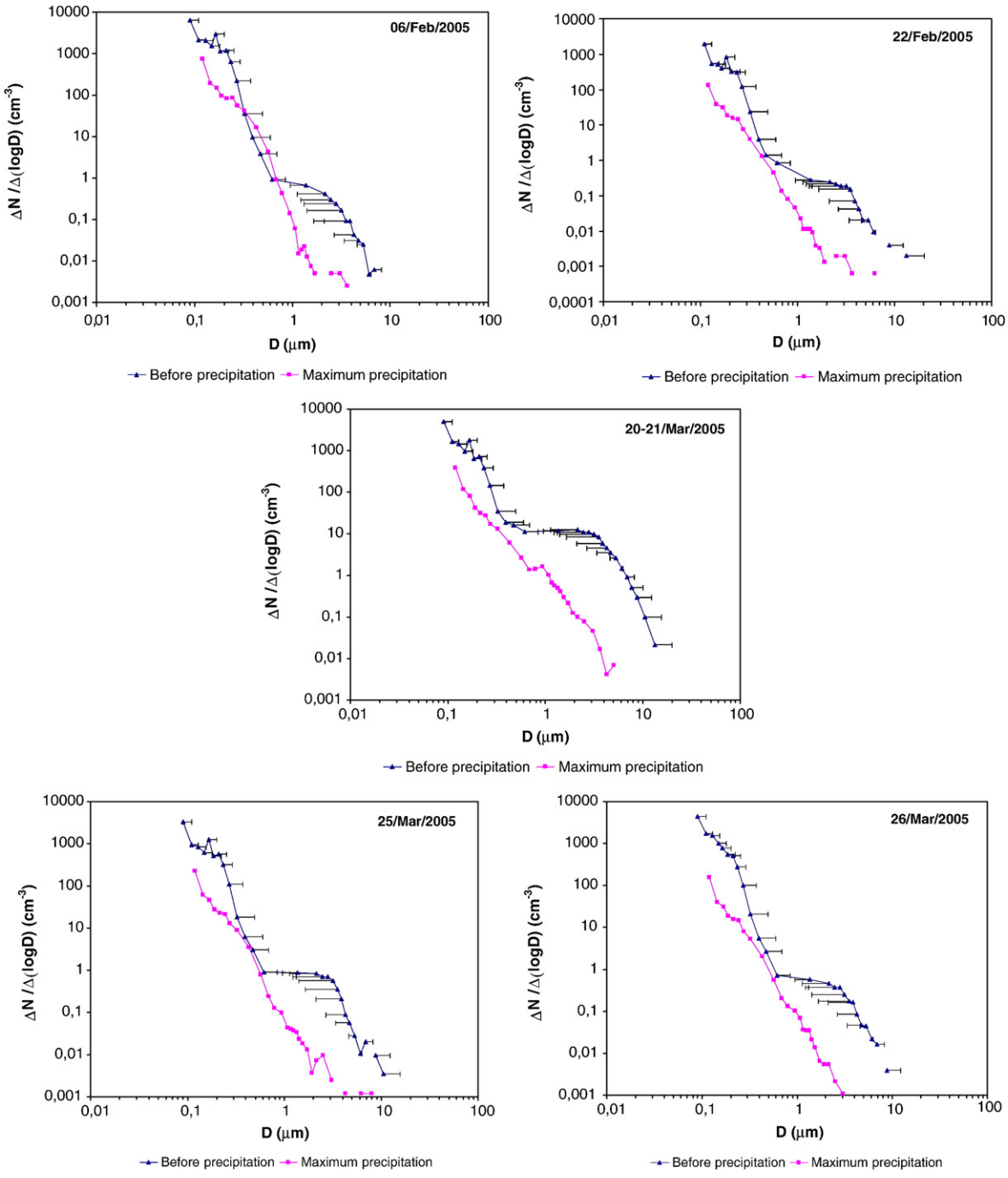

Fig. 7. Aerosol size distributions of each day with a rain event before and during the time interval of maximum precipitation with intensities of over 3.2 mm/h. The horizontal error bars represent the uncertainty in the size of the aerosol due to the variation of the refraction index between a dry and humid atmosphere.

measured increases, but this increase is smaller when the intensity of the precipitation increases ($r = -0.443$ with a significance level of $\alpha = 0.05$). As explained above, other aerosols are not likely to be incorporated while rain is falling because the air masses have not changed noticeably. Neither are there any known sources of aerosols around the probe that could be responsible for this sudden increase in the mean particle size. We therefore believe that the increase in size occurs because the probe is measuring on the one hand the aerosols in the air mass, and on the other hand small precipitating droplets or minute droplets in suspension. During the precipitation, as seen in Fig. 8, it may be seen that the number of particles larger than 1.3 μm decreases, which could lead to

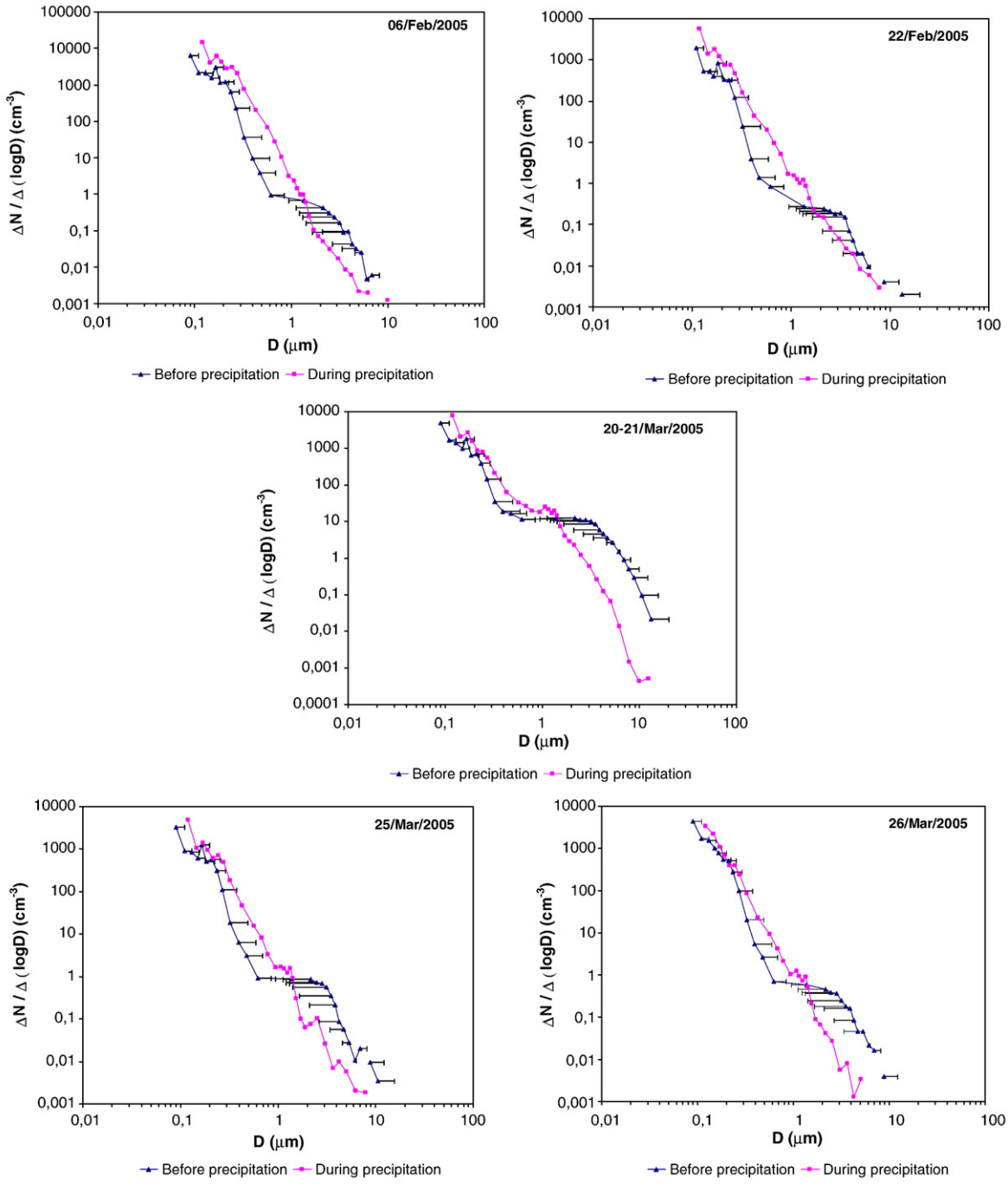

Fig. 8. Aerosol size distributions of each day with a rain event before and during the total interval of precipitation. The horizontal error bars represent the uncertainty in the size of the aerosol due to the variation of the refraction index between a dry and humid atmosphere.

a reduction in the average particle size. However, we should not forget that there are very few particles of these sizes, and therefore their contribution to the mean size is small. Also, the highest increase in the number of particles is recorded for those of less than 1.3 μm. The reasons for the increase in size may be, on the one hand, that the aerosols from the air mass have undergone hygroscopic growth as a result of collision and coalescence with rain droplets or the absorption of water vapor in the atmosphere (high relative humidity during the rain event). On the other hand, the particles may also increase in size due to collision and coagulation with the other aerosol particles. Finally, the small precipitating droplets or minute droplets in suspension that appear in the

Table 5
Mean values during the rain events of N, CMD, and σ_g and their standard deviations for the accumulation mode (f) and the coarse mode (c) of the number size distribution.

Number size distribution							
Measurement		Accumulation mode			Coarse mode		
		N_f (cm^{-3})	CMD_f (μm)	σ_{gf}	N_c (cm^{-3})	CMD_c (μm)	σ_{gc}
Before		500 ± 200	0.14 ± 0.00	1.45 ± 0.03	1.0 ± 1.9	2.23 ± 0.15	1.37 ± 0.08
During Precipitation	Maximum precipitation	400 ± 400	0.17 ± 0.01	1.48 ± 0.08	0.9 ± 1.7	2.34 ± 0.18	1.48 ± 0.08
	Other moments	1000 ± 1200	0.19 ± 0.01	1.43 ± 0.03	0.9 ± 1.5	2.28 ± 0.17	1.41 ± 0.11
After		600 ± 600	0.14 ± 0.01	1.45 ± 0.06	0.5 ± 0.8	2.42 ± 0.25	1.40 ± 0.08

precipitation may also be responsible for this increase in size. It must be taken into account that the study is restricted to the measuring range of the PCASP-X probe used, and that these other particles measured have a range of sizes similar to the range of aerosols in the atmosphere, but of somewhat larger sizes, on average, as the mean geometric diameter increased by 15% during the precipitation.

4.4. Multi-lognormal size, surface and volume distributions and precipitation

The size range of particles measured using PCASP-X provided only two modes (accumulation mode, for particles measuring between 0.1 and 1 μm, and coarse mode for particles larger than 1 μm). However, aerosols in the first three channels could correspond to larger diameters in a third mode, the Aitken mode, which we cannot describe here because there are insufficient data.

These two modes, accumulation and coarse, have been taken into consideration for this study and number, surface and volume distributions effectively show a bimodal profile. The study of these modes will enable us to analyze the performance of the lognormal distributions of the measurements carried out before, during and after the rain event, and to detect the range of sizes where changes have occurred.

Tables 5–7 show the results found for the lognormal distributions in both modes, accumulation and coarse: *N*, CMD and σ_g for number size distribution, *S*, SMD and σ_g for surface distribution and *V*, VMD and σ_g for volume distribution.

The results reveal that in the accumulation mode the number of particles cm^{-3} grows with precipitation, increasing on average from 500 particles cm^{-3} to 1000 particles cm^{-3}, except when the intensity of the precipitation is the maximum registered, with 400 particles m^{-3}, revealing an evident washout effect under these conditions. In other words, if we consider that the air mass does not change and no extraordinary contribution of aerosols seems likely, the probe is detecting small rain droplets that lead to an overestimation in the number of aerosols detected by the probe during rain events. Also, as in the case of the total distribution studied in the previous section, in this accumulation mode, even an hour and a half after the rain has ceased, the number of particles is slightly higher than the number of particles in the atmosphere before the rain began. Before raining, there was an average of 500, and afterwards, an average of 600 particles cm^{-3}. Apparently, the atmosphere gradually returns to its initial condition.

We consider that the increase in the number of particles recorded during the rainfall event is not due to droplet shatter, as the sampling volume of the PCASP is far from any region where this could occur, and also that the probability of droplet shatter on the outside of the PCASP probe should be independent from the precipitation intensity, and the measurements indicate that a higher concentration of particles is recorded in situations with a lower precipitation intensity.

But even though in the accumulation mode the particle size before and after the precipitation is 0.14 μm, during the rain event the diameter grows to 0.19 μm (meaning an increase of 36%), i.e., during rain the probe detects more particles and these particles are larger than the ones registered before the rain. The mean size of particles measured is of 0.17 μm in the moment of maximum intensity of the precipitation.

In the coarse mode the mean diameters are around 2 μm and the number of particles is very small, hardly 1 particle cm^{-3}. The increase in particle size affects mainly

Table 6
Mean values during the rain events of *S*, SMD, and σ_g and their standard deviations for the accumulation mode (a) and the coarse mode (c) of the surface distribution.

Measurement		Surface distribution					
		Accumulation mode			Coarse mode		
		S_a (μm^2 cm^{-3})	SMD_a (μm)	σ_{ga}	S_c (μm^2 cm^{-3})	SMD_c (μm)	σ_{gc}
Before		38 ± 17	0.16 ± 0.01	1.41 ± 0.07	20 ± 40	2.93 ± 0.27	1.48 ± 0.26
During Precipitation	Maximum precipitation	32 ± 30	0.22 ± 0.02	1.43 ± 0.08	20 ± 40	1.68 ± 0.16	1.46 ± 0.13
	Other moments	90 ± 120	0.21 ± 0.02	1.45 ± 0.08	30 ± 50	1.67 ± 0.19	1.53 ± 0.18
After		50 ± 50	0.14 ± 0.02	1.42 ± 0.08	10 ± 30	3.0 ± 0.2	1.43 ± 0.14

Table 7
Mean values during the rain events of V, VMD, and σ_g and their standard deviations for the accumulation mode (a) and the coarse mode (c) of the volume distribution.

Measurement		Volume distribution					
		Accumulation mode			Coarse mode		
		V_a (μm^3 cm^{-3})	VMD_a (μm)	σ_{ga}	V_c (μm^3 cm^{-3})	VMD_c (μm)	σ_{gc}
Before		1 ± 1	0.18 ± 0.01	1.38 ± 0.10	10 ± 30	3.23 ± 0.34	1.62 ± 0.59
During Precipitation	Maximum precipitation	1 ± 1	0.26 ± 0.01	1.54 ± 0.09	20 ± 30	2.74 ± 0.18	1.47 ± 0.04
	Other moments	3 ± 3	0.26 ± 0.01	1.47 ± 0.03	20 ± 40	2.78 ± 0.41	1.48 ± 0.06
After		2 ± 3	0.16 ± 0.02	1.44 ± 0.07	7 ± 16	3.32 ± 0.52	1.44 ± 0.11

the accumulation mode. The surface and volume distribution for the accumulation mode present a similar behavior during the rain event with values of S_f and V_f of 90 μm^2 cm^{-3} and 3 μm^3 cm^{-3}, respectively.

In consequence, the measurements carried out by an aerosol probe such as the one used in this study must be treated separately in the case of rainfall events with low precipitation intensities (of less than 0.6 mm/h), as we believe that the probe measures aerosols plus droplets of rain (instrumental artifacts). These special situations present the characteristics of a very dense fog or drizzle. However, if the precipitation exceeds 3.2 mm/h, the measurements for the concentration of aerosols are perfectly valid during a rainfall event. These preliminary results must still be confirmed in further studies.

5. Conclusions

In rain events of very low intensity (<0.6 mm/h) the probe of the laser spectrometer — PCASP-X — detects ambient aerosols but also small precipitating droplets and small droplets in suspension if their sizes fall within the range measured by the probe.

It has been observed that when the precipitation intensity exceeds 3.2 mm/h the washout is fast and noticeable, and the number of ambient particles decreases, large and small particles alike.

A negative correlation has been found between the intensity of the precipitation and the geometric mean diameter, i.e., during a rain event the mean diameter of the particles measured increases, but the higher the intensity of the precipitation, the smaller the increase.

In the case of weak precipitation of 0.6 mm/h or less, the number of particles increases considerably: up to seven times the number of particles detected by the probe with average sizes larger than the ones registered before the beginning of the rain event, from 0.39 μm to 0.45 μm. In other words, there was a lot of variation in the distributions and the number of particles smaller than 1.3 μm increases, whereas the number of particles larger than 1.3 μm decreases. This may be due to the fact that the probe does not discriminate between aerosols and very small precipitating droplets or the smallest droplets that are left in suspension in the atmosphere.

The authors believe that the measurements carried out using the aerosol probe used in this study must be treated separately for the case of weak rain (R<0.6 mm/h) days and for the case of days with more intense rain (R>3.2 mm/h) or without rain.

Acknowledgements

The authors are grateful to Antonio Ortín and Toyi del Canto for their cooperation and to Dr. Noelia Ramón for translating the paper into English. Also, the authors would like express their gratitude to the NASA/Goddard Space Flight Center, NOAA Air resources Laboratory, Naval Research Laboratory for the HYSPLIT transport model. Many thanks go to the researchers in the Project CALIMA for making their studies available. These data have been provided as a result of a joint research project for the study and assessment of atmospheric pollution by particulate matter in suspension in Spain, a project involving the Spanish Ministry of the Environment, the National Research Board and the National Agency of Meteorology (http://www.calima.ws). This study was supported by CICYT (grant TEC2007-63216) and the Regional Government Junta de Castilla y León (LE014A07). The authors are especially indebted to Dr. Darrel Baumgardner, from the Center of Atmospheric Sciences UNAM (Mexico), for his technical and scientific support.

References

Aklilu, Y., Mozurkewich, M., Prenni, A.J., Kreidenweis, S.M., Alfarra, M.R., Allan, J.D., Anlauf, K., Brook, J., Leaitch, W.R., Sharma, S., Boudries, H., Worsnop, D.R., 2006. Hygroscopicity of particles at two rural, urban influenced sites during Pacific 2001: comparison with estimates of water uptake from particle composition. Atmos. Env. 40, 2650–2661.

Birmili, W., Wiedensohler, A., Heintzenberg, J., Lehmann, K., 2001. Atmospheric particle number size distribution in central Europe: statistical relations to air masses and meteorology. J. Geophys. Res. 106, 32 005–32 018.

Bohren, C.F., Huffman, D.R., 1983. Absorption and Scattering of Light by Small Particles. Wiley, New York.

Busch, B., Kandler, K., Schütz, L., Neusüß, C., 2002. Hygroscopic properties and water-soluble volume fraction of atmospheric particles in the diameter range from 50 nm to 3.8 mm during LACE 98. J. Geophys. Res. 107 (D21), 8119.

Cocker, D.R., Whitlock, N.E., Flagan, R.C., 2001. Hygroscopic properties of Pasadena, California aerosol. Aerosol Sci. Technol. 35, 637–647.

Collins, D.R., Jonsson, H.H., Seinfeld, J.H., Flagan, R.C., Gasso, S., Hegg, D.A., Russell, P.B., Schmid, B., Livingston, J.M., Ostrom, E., Noone, K.J., Russell, L. M., Putaud, J.P., 2000. In situ aerosol-size distributions and clear-column radiative closure during ace-2. Tellus Series B—Chem. Phys. Meteor. 52, 498.

Dana, M.T., 1971. Washout of soluble dye particles. Pacific Northwest Laboratory Annual Report for 1970 to the USAEC Division of Biology and Medicine. Vol. II. : In: Simpson, et al. (Ed.), Physical Science. Part I. Atmospheric Sciences, USAEC Report BNWL-1551. Battelle Pacific Northwest Laboratories, pp. 63–67.

Dana, M.T., 1972. Washout of Rhodamine dye particles. In: David, H.S. (Ed.), Meteorology and Atomic Energy — 1968. USAEC Report TID-24190. Environmental Science Services Administration, NTIS, pp. 36–44.

Dana, M.T., Hales, J.M., 1976. Statistical aspects of the washout of polydisperse aerosols. Atmos. Env. 10, 45–50.

Draxler, R.R., Hess, G.D., 1998. An overview of the HYSPLIT_4 modelling system for trajectories, dispersion and deposition. Aust. Met. Mag. 47, 295–308.
Draxler, R.R., Rolph, G.D., 2003. HYSPLIT (HYbrid Single-Particle Lagrangian Integrated Trajectory). Model access via NOAA ARL READY Website (http://www.arl.noaa.gov/ready/hysplit4.html). NOAA Air Resources Laboratory, Silver Spring, MD.
Guyon, P., Boucher, O., Graham, B., Beck, J., Mayol-Bracero, O.L., Roberts, G.C., Maenhaut, W., Artaxo, P., Andreae, M.O., 2003. Refractive index of aerosol particles over the Amazon tropical forest during LBA-EUSTACH 1999. Aerosol Sci. 34, 883–907.
Hinds, W.C., 1999. Aerosols Technology: Properties, Behaviour and Measurement of Airborne Particles, 2nd Ed. Wiley, New York.
Hoppel, W.A., Frick, G.M., Fitzgerald, J., Larson, R.E., 1994. Marine boundary-layer measurements of new particle formation and the effects non-precipitating clouds have on aerosol size distribution. J. Geophys. Res. 99, 14 443–14 459.
Huebert, B.J., Zhuang, L., Howell, S., Noone, K., Noone, B., 1996. Sulphate, nitrate, methanesulfonate, chloride, ammonium and sodium measurements from ship, island and aircraft during the Atlantic stratocumulus transition experiment/ma-rine aerosol gas exchange. J. Geophys. Res. 101, 4413–4423.
Hussein, T., Hämeri, K., Aalto, P.P., Paatero, P., Kulmala, M., 2005. Modal structure and spatial-temporal variations of urban and suburban aerosols in Helsinki—Finland. Atmos. Env. 39, 1655–1668.
Ito, T., 1993. Size distribution of Antarctic submicron aerosols. Tellus 45, 145–159.
Jenkinson, A.F., Collison, F.P., 1977. An initial climatology of gales over the North Sea. Synoptic Climatology Branch Memorándum, 62. Meteorological Office, London.
Jirak, I.L., Cotton, W.R., 2006. Effect of air pollution on precipitation along the front range of the rocky mountains. J. Appl. Meteor. Climatol. 45, 236–245.
Jonses, P.D., Hulme, M., Briffa, K.R., 1993. A comparison of Lamb circulation types with an objective classification scheme. Int. J. Climatol. 13, 655–663.
Kerminen, V.-M., 1997. The effects of particle chemical character and atmospheric processes on particle hygroscopic properties. J. Aerosol Sci. 28, 121–132.
Kerminen, V.-M., Wexler, A.S., 1995. Growth laws for atmospheric aerosol particles: an examination of the bimodality of the accumulation mode. Atmos. Env. 29, 3263–3275.
Kim, Y.J., Boatman, J.F., 1990. Size calibration corrections for the active scattering aerosol spectrometer probe (ASASP-100X). Aerosol Sci. Technol. 12 (3), 665–672.
Lamb, H.H., 1972. British Isles weather types and a register of daily sequence of circulation patterns, 1861–1971. Geophysical Memoir 116. HMSO, London.
Lide, D.R., 1993. Handbook of Chemistry and Physics, CRC, Boca Raton, pp. 6–193. 74th Edn. ed.
Mäkelä, J.M., Koponen, I., Aalto, P., Kulmala, M., 2000. One-year data of submicron size modes of tropospheric background aerosolin southern Finland. J. Aerosol Sci. 31, 595–611.
Mircea, M., Stefan, S., Fuzzi, S., 2000. Precipitation scavenging coefficient: influence of measured aerosol and raindrop size distributions. Atmos. Env. 34, 5169–5174.
Peng, C., Chan, M.N., Chan, C.K., 2001. The hygroscopic properties of dicarboxylic and multifunctional acids: measurements and UNIFAC predictions. Env. Sci. Tech. 35 (22), 4495–4501.
Slinn, W.G.N., 1971. Numerical explorations of washout of aerosol particles. Pacific Northwest Laboratory Annual Report for 1070 to the USAEC Division of Biology and Medicine, Vol. II. : In: Simpson, et al. (Ed.), Physical Sciences, C.L. USAEC Report BNWL-1751 (Part. 1). Battelle Pacific Northwest Laboratory, pp. 75–81.
Suzuki, T., Tsunogai, S., 1988. Daily variation of aerosols of marine and continental origin in the surface air over a small island Okushin in Japan sea. Tellus 40, 42–49.
Swietlicki, E., Zhou, J., Berg, O.H., Martinsson, B.G., Frank, G., Cederfelt, S., Dusek, U., Berner, A., Birmili, W., Wiedensohler, A., Yuskiewicz, B., Bower, K.N., 1999. A closure study of sub-micrometer aerosol particle hygroscopic behavior. Atmos. Res. 50, 205–240.
Teller, A., Levin, Z., 2006. The effects of aerosols on precipitation and dimensions of subtropical clouds: a sensitivity study using a numerical cloud model. Atmos. Chem. Phys. 6, 67–80.
Trigo, R.M., DaCamara, C.C., 2000. Circulation weather types and their influence on the Precipitación Regime IN Portugal. Int. J. Climatol. 20, 1559–1581.
Väkevä, M., Hameri, K., Puhakka, T., Nilsson, E.D., Hohti, H., Mäkelä, J.M., 2000. Effects of meteorological processes on aerosol particle size distribution in an urban background area. J. Geophys. Res. 105, 9807–9821.
Väkevä, M., Kulmala, M., Strarmann, F., Hämeri, K., 2002. Field measurements of hygroscopic properties and state of mixing of nucleation mode particles. Atmos. Chem. Phys. 2, 55–66.
Whitby, K.H., 1978. The physical characteristics of sulphur aerosols. Atmos. Env. 12, 135–159.